

The ηNN -system at low energy within a three-body approach*

A. Fix[†] and H. Arenhövel

Institut für Kernphysik, Johannes Gutenberg-Universität, D-55099 Mainz, Germany

(October 26, 2018)

The role of the ηNN -interaction is studied in the low energy regime in η -deuteron reactions as well as in coherent and incoherent η -photoproduction on the deuteron using a three-body model with separable two-body interactions. The three-body approach turns out to be quite essential in the most important lowest partial wave. Results are presented for differential and total cross sections as well as for the η -meson spectrum. They differ significantly from those predicted by a simple rescattering model in which only first-order ηN - and NN -interactions in the final state are considered. The major features of the experimental data of η -photoproduction in the near-threshold region are well reproduced.

PACS numbers: 13.60.Le, 21.45.+v, 25.20.Lj

I. INTRODUCTION

The basic phenomenon, which plays a crucial dynamical role in medium energy physics, is the excitation of baryon resonances inside a nucleus, either in a hadronic or an electromagnetic reaction. The phenomenological framework, in which the nuclear dynamics in this energy region is described, is in terms of a series of excitations and subsequent decays of baryon resonances in a nuclear medium with intermediate meson exchange.

A particularly interesting topic is the field of η -meson physics, because the ηN -interaction is dominated at low energy by the almost exclusive coupling to the $N^*(1535)$ -resonance. Thus the η -nucleus dynamics is shifted to that of the $N^*(1535)$, i.e., to the N^* -nucleus interaction. The essential question is, how well do we understand this interaction. Until now, the N^* -nucleus dynamics has been treated either purely phenomenological within the N^* -hole model [1,2] or by combining microscopic and phenomenological tools in the so called local density approximation [3,4] or using the BUU model [5]. However, such approaches leave open the question of the underlying “elementary” N^*N -interaction in few body systems, where one must go beyond the simplified approaches for the N^* -dynamics in nuclear matter. The present investigation is an attempt to shed some light on this particular problem by studying elastic and inelastic η -deuteron scattering as well as η -photoproduction on the deuteron.

Elastic ηd -scattering at low energy has been considered recently in [6–9], mainly in connection with a search for rather exotic bound ηd -states. The outstanding feature of the ηd -interaction, found in all analyses, is its strong energy dependence which manifests itself in the sharp enhancement of the cross section near zero energy. The origin of this feature is a pole in the s -wave scattering amplitude near the physical region. However, despite all theoretical efforts, using rather nontrivial models, even a qualitative understanding of the low-energy ηd -interaction has not been reached. In fact, the different results show a strong qualitative disagreement which cannot be explained alone by the large uncertainties in our knowledge of the ηN low-energy interaction. For example, in [8,10] the existence of an ηd s -wave resonance was claimed, which, however, was not observed by other authors [9,11,12]. The authors of [9] have found that weakening the strength of the ηN -forces implies the disappearance of the quasibound state without generating an ηd -resonance, while the strong enhancement of the cross section remains. Recently, we have shown in [12] that it is very likely, that the strong energy dependence of the ηd -scattering amplitude is generated by a virtual state into which the bound state turns by weakening the ηN -interaction strength. We also would like to point out that our conclusion agrees with the one given in [11], where the three-body equations have been solved by the partial summation of the multiple scattering series.

Also the role of pion exchange in the N^*N -interaction remains unclear. The results shown in [13] support a very strong damping of the attraction in the ηd -system due to π -exchange. On the other hand, in [12] this effect was found to be insignificant. Therefore, the physics of low-energy ηd -interaction is by no means understood, and further careful studies are required.

*Supported by the Deutsche Forschungsgemeinschaft (SFB 443)

[†]Permanent address: Tomsk Polytechnic University, 634034 Tomsk, Russia

In the present paper we will continue and extend our study of the ηNN -system of [12,14]. It is reasonable to expect that the virtual poles in the ηNN -scattering matrix found in [12] would have important consequences for elastic and inelastic ηd -scattering in the energy region of a few MeV above threshold. This is the region which we wish to explore in this paper, and it is our purpose to survey those important features of the ηNN -interaction, which are expected to influence the η -production reactions. We would like to note that due to rather large uncertainties of the experimental input on the one hand and a very strong model dependence on the theory side, a considerable freedom remains in fitting the isobar ansatz for the ηN - πN - $\pi\pi N$ coupled channel system to the low energy data. As a consequence, the results for the ηN -scattering length range from $a_{\eta N} = (0.27 + 0.22i)$ fm [15] to $a_{\eta N} = (0.88 + 0.27i)$ fm [16]. In this connection we think that it is very hard at present to make precise quantitative statements about the character of the ηd low-energy interaction based on the coupled channel approach alone. Therefore, we will focus our attention primarily on the qualitative aspects of this phenomenon which, we believe, are more or less independent of future refinements of the ηN -dynamics, when more theoretical and experimental material will be available.

Information obtained from photon-induced η -production may be considered as complementary to that from ηd -scattering. Indeed, due to the large momentum transfer, the η -photoproduction cross section is closely connected with the high momentum part of the N^*N -interaction, which, as we will see, is only of minor importance in the low-energy ηd -scattering. Photoproduction reactions $\gamma d \rightarrow \eta d$ and $\gamma d \rightarrow \eta np$ have been extensively studied over recent years in [10,17,39,19–21]. The interest in these reactions is motivated by two main reasons. Firstly, one has the possibility to extract information about the η -photoproduction strength on a neutron within the framework of a detailed microscopic approach. This question is closely connected with the problem of the isotopic separation of the N^* -photoexcitation amplitude discussed, e.g., in [21–24]. Secondly, these reactions permit a nondirect investigation of the N^*N -interaction in different spin-isospin channels. In the spirit of our theoretical focus, we will pay our attention mostly to the second aspect.

Thus we will consider in this work the N^*N -interaction as an ηNN three-body problem. We would like to note, that the study of the N^*N -interaction in analogy to the familiar NN two-body potential scattering, i.e., treating the N^* essentially as a stable particle, would be incorrect. This is because of large retardation effects expected, e.g., in the ηNN channel, to which the N^*N -system is coupled, leading to a strong nonlocality of the N^*N -interaction. Therefore, any realistic approach must include explicitly meson degrees of freedom. This aspect may unambiguously be taken into account in the framework of a three-particle model, where special theoretical techniques are available for solving the appropriate dynamical equations.

Before dealing with the main subject, we describe in Sect. II the essential ingredients of the formalism used in the present study. The three-body equations are simplified without loss of essential physics by using separable potentials for the two-body forces. We also pay some attention to the explicit inclusion of the absorptive πNN channel. We then specialize in Sect. III to the problem of ηd -scattering which, although experimentally not accessible, supplies the important input for the subsequent treatment of η -production. In Sect. IV the consequences on the break-up reactions arising from unitarity are considered. Photoproduction is treated in Sect. V where we will compare the present calculation to recent experimental data for the coherent and incoherent reactions $\gamma d \rightarrow \eta d$ and $\gamma d \rightarrow \eta np$. We will show, that the main features of the ηNN -system, predicted by our model are in rather good agreement with these measurements. The last Section VI is devoted to conclusions. Here, we will also address some questions concerning the N^* -nuclear dynamics and possible mechanisms of η -meson production on heavier nuclei in the near-threshold region.

II. FORMALISM

In this section we briefly review the basic features of three-body techniques for the application to the ηNN -dynamics. The system under consideration consists of two nucleons, N_1 and N_2 , and an η -meson, which will be denoted as particle 1,2 and 3, respectively. In the c.m. frame the basic free particle states $|\vec{p}_i, \vec{q}_i\rangle$ will be characterized as usual by a pair of vectors \vec{p}_i and \vec{q}_i , where \vec{p}_i is the relative momentum of a (jk) -pair ($j \neq i \neq k$) and \vec{q}_i denotes the relative momentum of the unpaired particle i with respect to the c.m. frame of the pair.

In order to approximate the three-body equations in such a way that they become practically solvable, it is customary to introduce a separable ansatz for each two-body interaction. In our case this approximation has also a physical motivation because of the strong dominance of the s -wave pole terms in the low-energy ηN - and NN -scattering matrices. Thus we will assume that the two-body driving forces can be approximated by rank-one potentials, which, when regarded as operators in the three-body Hilbert space, have the form

$$v_i = \gamma_i \int \frac{d^3q}{(2\pi)^3} |i, \vec{q}\rangle \langle i, \vec{q}|, \quad (1)$$

with i being the channel index, in detail

$$|i, \vec{q}\rangle = \left\{ \begin{array}{l} |N_1(\vec{q}), (N_2\eta)\rangle \text{ for } i = 1 \\ |N_2(\vec{q}), (N_1\eta)\rangle \text{ for } i = 2 \\ |\eta(\vec{q}), (N_1N_2)\rangle \text{ for } i = 3 \end{array} \right\}. \quad (2)$$

Here the ket $|i, \vec{q}\rangle = |i\rangle \otimes |\vec{q}\rangle$ is defined such that

$$\langle \vec{p}, \vec{q} | i, \vec{q}' \rangle = \langle \vec{p} | i \rangle \langle \vec{q} | \vec{q}' \rangle = (2\pi)^3 \epsilon_i(\vec{q}) \delta(\vec{q} - \vec{q}') f_i(\vec{p}) \quad \text{with} \quad \epsilon_i(\vec{q}) = \left\{ \begin{array}{l} 2E_i(\vec{q}) \text{ for } i = 3 \\ \frac{E_i(\vec{q})}{M_N} \text{ for } i = 1, 2 \end{array} \right\}, \quad (3)$$

where $f_i(\vec{p}) = \langle \vec{p} | i \rangle$ is the usual vertex function of the separable representation. For $i = 3$ the Pauli principle for the nucleons is already incorporated, i.e., $P_{12}|3, \vec{q}\rangle = -|3, \vec{q}\rangle$ where P_{12} is the nucleon exchange operator.

The asymptotic channel wave function, describing the free motion of a particle “ i ” with momentum \vec{q} relative to the interacting pair (jk) , is given by

$$|\phi_i(W, \vec{q})\rangle = G_{\eta NN}(W)|i, \vec{q}\rangle, \quad (4)$$

where $G_{\eta NN}(W)$ is the free ηNN Green’s function depending on the total three-body energy W . For the moment being we drop spin-isospin indices. Then, expressing the separable ηN - and NN -scattering matrices, acting in three-particle space, in terms of the two-body matrix elements, we find

$$\langle \vec{p}', \vec{q}' | t_i(W) | \vec{p}, \vec{q} \rangle = (2\pi)^3 \delta(\vec{q}' - \vec{q}) \langle \vec{p}' | t_i(W_i(W, \vec{q})) | \vec{p} \rangle = (2\pi)^3 \delta(\vec{q}' - \vec{q}) f_i^*(\vec{p}') \tau_i(W_i(W, \vec{q})) f_i(\vec{p}), \quad (5)$$

where the propagator of a pair (jk) in the presence of a spectator “ i ” reads

$$\tau_i(W_i) = \left[\frac{1}{\gamma_i} - \frac{1}{(2\pi)^3} \int \frac{d^3 p}{\epsilon_j(\vec{p}) \epsilon_k(\vec{p})} \frac{|f_i(\vec{p})|^2}{W_i - E_j(\vec{p}) - E_k(\vec{p}) + i\epsilon} \right]^{-1}. \quad (6)$$

Here $W_i(W, \vec{q})$ denotes the invariant mass of the subsystem (j, k) , defined by putting the spectator particle “ i ” on mass shell, i.e.

$$W_i(W, \vec{q}) = \sqrt{W^2 - 2W E_i(\vec{q}) + M_i^2}. \quad (7)$$

For the particle energies we use the relativistic expressions $E_i(\vec{p}) = \sqrt{p^2 + M_i^2}$. The separable ansatz leads to a system of coupled equations of the familiar Lippman-Schwinger form [25]

$$X_{ij}(W, \vec{q}', \vec{q}) = Z_{ij}(W, \vec{q}', \vec{q}) + \sum_{k=1}^3 \int \frac{d^3 q''}{(2\pi)^3 \epsilon_k(q'')} Z_{ik}(W, \vec{q}', \vec{q}'') \tau_k(W_k(W, \vec{q}'')) X_{kj}(W, \vec{q}'', \vec{q}). \quad (8)$$

The amplitudes $X_{ij}(W)$ define the transitions between the channel states (2), i.e. collisions of the type “ $j + (ik) \rightarrow i + (jk)$ ”, where (ik) and (jk) refer to interacting two-particle states. The driving terms $Z_{ij}(W)$ are represented by the matrix elements of the free ηNN Green’s function

$$Z_{ij}(W, \vec{q}', \vec{q}) = (1 - \delta_{ij}) \langle i, \vec{q}' | G_{\eta NN}(W) | j, \vec{q} \rangle. \quad (9)$$

Explicitly one finds for $i \neq j$

$$Z_{ij}(W, \vec{q}', \vec{q}) = \frac{f_i^*(\vec{p}_i(\vec{q}', \vec{q})) f_j(\vec{p}_j(\vec{q}', \vec{q}))}{W - E_i(\vec{q}') - E_j(\vec{q}) - E_k(\vec{q}' + \vec{q}) + i\epsilon}, \quad (10)$$

where the momenta $\vec{p}_i(\vec{q}', \vec{q})$ and $\vec{p}_j(\vec{q}', \vec{q})$ are given in terms of \vec{q}' and \vec{q} . For simplicity we use the nonrelativistic relations

$$\vec{p}_i(\vec{q}', \vec{q}) = \vec{q} + \frac{\mu_i}{M_k} \vec{q}' \quad \text{and} \quad \vec{p}_j(\vec{q}', \vec{q}) = \vec{q}' + \frac{\mu_j}{M_k} \vec{q}, \quad (11)$$

where the reduced mass in i -th channel reads

$$\mu_i = \frac{M_j M_k}{M_j + M_k}. \quad (12)$$

The next step to be taken towards an explicit evaluation of the three-body equations is the antisymmetrization of the basic amplitudes with respect to the exchange of the nucleons N_1 and N_2 for which we follow mainly the work of [26]. It affects only the channels $i = 1$ and $i = 2$ because the channel $i = 3$ is already antisymmetric by construction as pointed out above. Consider the system of equations, which couple the amplitudes X_{ij} for the possible transitions from the channel $j = 3$. In the operator form we have explicitly

$$\begin{aligned} X_{13} &= Z_{13} + Z_{12} \tau_2 X_{23} + Z_{13} \tau_3 X_{33}, \\ X_{23} &= Z_{23} + Z_{21} \tau_1 X_{13} + Z_{23} \tau_3 X_{33}, \\ X_{33} &= Z_{31} \tau_1 X_{13} + Z_{32} \tau_2 X_{23}. \end{aligned} \quad (13)$$

Taking into account the identity of the nucleons, it is easy to find the following relations [26]

$$\tau_1 = \tau_2, \quad Z_{13} = -Z_{23}, \quad Z_{31} = -Z_{32}, \quad \text{and} \quad Z_{12} = Z_{21}. \quad (14)$$

With the help of this symmetry one can reduce (13) to a system of only two coupled equations

$$(X_{13} - X_{23}) = 2Z_{13} - Z_{12} \tau_2 (X_{13} - X_{23}) + 2Z_{13} \tau_3 X_{33}, \quad (15)$$

$$X_{33} = Z_{31} \tau_1 (X_{13} - X_{23}). \quad (16)$$

Before defining the explicitly antisymmetrized amplitudes, it is convenient to introduce a new channel notation. From now on we denote the channel with a spectator nucleon as “ N^* ” and the one with a spectator meson as “ d ”. The corresponding channel wave functions $|N^*, \vec{q}\rangle$ and $|d, \vec{q}\rangle$ are assumed to be antisymmetrized with respect to the nucleons, in detail

$$|N^*, \vec{q}\rangle = \frac{1}{\sqrt{2}} (|1, \vec{q}\rangle - |2, \vec{q}\rangle) \quad \text{and} \quad |d, \vec{q}\rangle = |3, \vec{q}\rangle. \quad (17)$$

Defining the driving terms in a symbolic notation by

$$Z_{N^*N^*} = -\frac{1}{2}(Z_{12} + Z_{21}) = -Z_{12}, \quad Z_{dN^*} = Z_{31}, \quad \text{and} \quad Z_{N^*d} = Z_{13}, \quad (18)$$

and the properly antisymmetrized amplitudes by

$$X_d = X_{33}, \quad X_{N^*d} = \frac{1}{2} (X_{13} - X_{23}), \quad (19)$$

one arrives at the following set of equations

$$X_{N^*d} = Z_{N^*d} + Z_{N^*d} \tau_d X_d + Z_{N^*N^*} \tau_{N^*} X_{N^*d}, \quad (20)$$

$$X_d = 2 Z_{dN^*} \tau_{N^*} X_{N^*d}, \quad (21)$$

where the amplitudes X_d and X_{N^*d} describe the two different transitions $\eta d \rightarrow \eta d$ and $\eta d \rightarrow N^*N$, respectively, which are realized in ηd scattering.

Now we will consider in addition the coupling to the πNN channel via the two-body reaction $\eta N \rightarrow \pi N$, whereas we will neglect the coupling to the two-pion channel $\pi\pi NN$. Its inclusion into the three-body formalism would require the use of phenomenological approaches, which in any case seem to be very ambiguous. Due to the smallness of the $N^* \rightarrow \pi\pi N$ decay probability we believe that this neglect will not significantly influence our results. A treatment of the resulting coupled channel problem within the Faddeev approach was developed, e.g., in [27,28]. Accordingly, we extend the channel $|N^*\rangle$ to the following two-component form

$$|N^*\rangle = \begin{pmatrix} |N^*(\eta)\rangle \\ |N^*(\pi)\rangle \end{pmatrix}. \quad (22)$$

The corresponding coupled channel t -matrix is given by

$$t_{N^*} = |N^*\rangle \tau_{N^*} \langle N^*|, \quad (23)$$

with the N^* -propagator

$$\tau_{N^*}(W_{N^*}) = \left[\frac{1}{\gamma_{N^*}} - \frac{1}{(2\pi)^3} \sum_{\alpha \in \{\pi, \eta\}} \int \frac{M_N}{2 E_\alpha(\vec{p}) E_N(\vec{p})} \frac{|f_{N^*}^{(\alpha)}(\vec{p})|^2}{W_{N^*} - E_N(\vec{p}) - E_\alpha(\vec{p}) + i\epsilon} d^3p \right]^{-1}, \quad (24)$$

where $f_{N^*}^{(\alpha)}(\vec{p}) = \langle \vec{p} | N^*(\alpha) \rangle$. Turning now to the three-body problem, we obtain a set of three coupled equations, namely

$$X_{N^*d} = Z_{N^*d}^{(\eta)} + Z_{N^*d}^{(\eta)} \tau_d^{(\eta)} X_d^{(\eta)} + Z_{N^*d}^{(\pi)} \tau_d^{(\pi)} X_d^{(\pi)} + (Z_{N^*N^*}^{(\eta)} + Z_{N^*N^*}^{(\pi)}) \tau_{N^*} X_{N^*d}, \quad (25)$$

$$X_d^{(\eta)} = 2 Z_{dN^*}^{(\eta)} \tau_{N^*} X_{N^*d}, \quad (26)$$

$$X_d^{(\pi)} = 2 Z_{dN^*}^{(\pi)} \tau_{N^*} X_{N^*d}, \quad (27)$$

where the driving terms are given in analogy to (18) for $\alpha \in \{\pi, \eta\}$ by

$$Z_{N^*N^*}^{(\alpha)} = -\frac{1}{2}(Z_{12}^{(\alpha)} + Z_{21}^{(\alpha)}), \quad Z_{dN^*}^{(\alpha)} = Z_{31}^{(\alpha)} \quad \text{and} \quad Z_{N^*d}^{(\alpha)} = Z_{13}^{(\alpha)}, \quad (28)$$

with analogous definitions for $Z_{ij}^{(\alpha)}$ as in (9), i.e.

$$Z_{ij}^{(\alpha)}(W, \vec{q}', \vec{q}) = (1 - \delta_{ij}) \langle i, \vec{q}' | G_{\alpha NN}(W) | j, \vec{q} \rangle. \quad (29)$$

The set of equations (25) through (27) is the formal basis of the present calculation. Its solution gives the required symmetrized rearrangement amplitudes and thus amounts to solving the ηNN -problem.

Now we will specify the separable ηN - and NN -scattering matrices which determine the driving two-body forces. Since we work entirely in the low-energy region we shall neglect all but the S_{11} - ηN -interaction. Analogously, only s -wave NN -states (1S_0 , 3S_1) are included in view of their strong dominance. As a first step, we omit the tensor part of the nucleon-nucleon force, because their inclusion would introduce further calculational complications. Since we restrict the pairwise interactions to s -waves only, the vertex functions have a very simple structure

$$\langle \vec{p} | k \rangle = f_k(\vec{p}) = g_k F_k(\vec{p}), \quad \text{with} \quad F_k(\vec{p}) = \frac{\beta_k^2}{\beta_k^2 + (\vec{p})^2}, \quad k \in \{d, N^*\}. \quad (30)$$

For the s -wave NN -scattering matrix

$$\langle \vec{p}' | t_d(W_d) | \vec{p} \rangle = f_d^*(\vec{p}') \tau_d(W_d) f_d(\vec{p}), \quad (31)$$

the following parametrization has been used

$$g_d^2 = \frac{16\pi a}{a\beta_d - 2}, \quad \gamma_d = -\frac{1}{2M_N}, \quad (32)$$

where a denotes the corresponding NN -scattering length. In order to simplify the numerical evaluations we reduce the function τ_d to the nonrelativistic form

$$\tau_d(E_{NN}) = -\frac{1}{2M_N} \left[1 + \frac{g_d^2 \beta_d^3}{16\pi (i\beta_d + \sqrt{M_N E_{NN}})^2} \right]^{-1}, \quad (33)$$

with E_{NN} being the kinetic NN -energy in their center of mass. To be more consistent one can, e.g., apply the minimal relativity to the separable nonrelativistic NN -amplitude, but we have checked that the results are not affected by the approximation (33).

The NN -interaction parameters were taken from a fit of low-energy np -scattering [29], yielding

$$\beta_d = 1.4488 \text{ fm}^{-1}, \quad a = \left\{ \begin{array}{l} 5.378 \text{ fm} \text{ for the } ^3S_1\text{-state} \\ -23.690 \text{ fm} \text{ for the } ^1S_0\text{-state} \end{array} \right\}. \quad (34)$$

For the N^* t -matrix (23) we use the energy dependent coupling strength $\gamma_{N^*} = (W_{N^*} - M_0)^{-1}$ so that the N^* -propagator is given in the familiar isobar form

$$\tau_{N^*}(W_{N^*}) = (W_{N^*} - M_0 - \Sigma_\pi(W_{N^*}) - \Sigma_\eta(W_{N^*}) + i\epsilon)^{-1}, \quad (35)$$

The self energy contributions $\Sigma_\alpha(W_{N^*})$ ($\alpha \in \{\pi, \eta\}$) from the πN - and ηN -loops are defined by the equation (24). The meson- N^* vertices are parametrized by

$$f_{N^*}^{(\alpha)}(\vec{p}) = g_{N^*}^{(\alpha)} F_{N^*}^{(\alpha)}(\vec{p}), \quad \text{with} \quad F_{N^*}^{(\alpha)}(\vec{p}) = \frac{\beta_{N^*}^{(\alpha)2}}{\beta_{N^*}^{(\alpha)2} + (\vec{p})^2}. \quad (36)$$

The small partial decay into the $\pi\pi N$ -channel has been neglected for consistency.

In the actual calculation we have chosen the following set of N^* -parameters

$$g_{N^*}^{(\eta)} = 2.0, \quad g_{N^*}^{(\pi)} = 1.1, \quad \beta_{N^*}^{(\eta)} = 6.5 \text{ fm}^{-1}, \quad \beta_{N^*}^{(\pi)} = 4.5 \text{ fm}^{-1}, \quad M_0 = 1622 \text{ MeV}, \quad (37)$$

which gives for the ηN -scattering length

$$a_{\eta N} = (0.75 + 0.27i) \text{ fm}^{-1}. \quad (38)$$

This value was obtained in [7] using a phenomenological analysis of the coupled channels πN , $\pi\pi N$, ηN and γN , and is in close agreement with other recent results for low-energy ηN -scattering [30].

In order to complete the formal part, we only have to generalize our formalism to add also spin-isospin degrees of freedom. Since we retain only s -wave orbitals for the two-body interactions, excluding in particular tensor forces, the total spin S is a good quantum number. Thus, we obtain the partial wave decomposition of the basic states as

$$|SM_S, TM_T, \vec{q}\rangle = |(\sigma_i \sigma_j) S_k \sigma_k; SM_S\rangle |(\tau_i \tau_j) T_k \tau_k; TM_T\rangle 4\pi \sum_{LM_L} |q, LM_L\rangle Y_{LM_L}(\hat{q}) \quad (39)$$

in a self explanatory notation for the coupling of the individual spins and isospins to S and T , respectively. In the basis of (39) the Born amplitudes are given by ($i, j \in \{d, N^*\}$)

$$Z_{ij}(W, \vec{q}', \vec{q}) = 4\pi \Lambda^{ST} \sum_L (2L+1) Z_{ij}^L(W, q', q) P_L(\hat{q}' \cdot \hat{q}), \quad (40)$$

where the driving term Z_{ij}^L of the partial wave L is defined by

$$Z_{ij}^L(W, q', q) = \frac{1}{8\pi} \int_{-1}^1 Z_{ij}(W, \vec{q}', \vec{q}) P_L(\hat{q}' \cdot \hat{q}) d(\hat{q}' \cdot \hat{q}). \quad (41)$$

The recoupling coefficients

$$\Lambda^{ST} = \langle (\sigma_i \sigma_j) S_k \sigma_k, S | (\sigma_j \sigma_k) S_i \sigma_i, S \rangle \langle (\tau_i \tau_j) T_k \tau_k, T | (\tau_j \tau_k) T_i \tau_i, T \rangle \quad (42)$$

are evaluated using the standard formula (see e.g. [31])

$$\langle (\sigma_i \sigma_j) S_k \sigma_k, S | (\sigma_j \sigma_k) S_i \sigma_i, S \rangle = (-1)^{\sigma_j + \sigma_k - S_i} \sqrt{(2S_i + 1)(2S_k + 1)} \begin{Bmatrix} \sigma_i & \sigma_j & S_k \\ \sigma_k & S & S_i \end{Bmatrix}, \quad (43)$$

and the analogous expression for the isospin recoupling. After a partial wave decomposition we have a system of coupled integral equations in only one variable, which schematically reads

$$X^{LST} = \Lambda^{ST} Z^L + \Lambda^{ST} Z^L \tau X^{LST}. \quad (44)$$

In the case of ηd scattering, only states with $T = 0$ and $S = 1$ contribute. But in η -photoproduction on the deuteron, other ST -combinations are realized.

In the Appendix we describe briefly the techniques involved to invert the system (25)-(27). The corresponding mathematical apparatus is quite standard by now, and we are concerned with some formal aspects only, connected with the relativistic kinematics explored in this paper.

III. ηd ELASTIC SCATTERING

The scattering amplitude is determined by the matrix element $X_d^{(\eta)}$ of (25)-(27) in the $(S = 1, T = 0)$ -channel

$$F_{\eta d}^L(q) = -\frac{E_d}{4\pi W} N_d^2 X_d^{(\eta)L}(W, q, q), \quad (45)$$

with q being the on-shell ηd c.m. momentum. The factor N_d takes into account the normalization of the deuteron wave function to unity. In our parametrization (32) we have

$$N_d^2 = 8\pi \frac{\epsilon_d^2}{g_d^2} \left(\frac{1}{\beta} + \frac{1}{\sqrt{M_N |\epsilon_d|}} \right)^3, \quad (46)$$

where ϵ_d is the deuteron binding energy. For the c.m. differential cross section one has the usual expression

$$d\sigma(\eta d \rightarrow \eta d) = \left| 4\pi \sum_L (2L+1) F_{\eta d}^L(q) P_L(\cos\theta) \right|^2 d\Omega. \quad (47)$$

We have calculated the scattering amplitudes for the first three partial waves, $L = 0, 1,$ and 2 . The results are summarized in Fig. 1, where the Argand plots as well as the corresponding inelasticity parameters η_L are presented. The following conclusions may be drawn:

(i) The rather rapid increase of the s-wave amplitude close to the scattering threshold is explained by the presence of a virtual pole in the $(S = 1, T = 0)$ ηd -state. This pole has been located in [12] on the nonphysical two-body sheet of the ηd c.m. kinetic energy plane. As is noted in the introduction, the existence of the virtual state leads to a strong enhancement of the scattering cross section, which is presented in Fig. 2.

(ii) With increasing energy the Argand plots show a resonance-like behaviour around the position of the elementary N^* -resonance. These ηd pseudoresonances are explained simply by the spreading of the elementary ηN -interaction over different partial waves when viewed from the ηd c.m.-system. In this energy region the amplitudes become highly inelastic, so that the scattering is almost diffractive. In the η -production reactions this effect appears as a strong absorption of the produced mesons inside the nucleus, leading to the so-called surface production mechanism [32].

(iii) The N^*N -interaction generated by pion exchange is almost negligible. This smallness is well understood if one takes into account the dominance of the low momentum part of the N^*N -interaction at low energy in on-shell ηd scattering. We expect that due to the smallness of the pion mass the exchange of the retarded pion determines mainly the high momentum component of $Z_{N^*N^*}$ in (25)

$$Z_{N^*N^*} \equiv Z_{N^*N^*}^{(\eta)} + Z_{N^*N^*}^{(\pi)} \quad (48)$$

and thus is not very important in our case. In this connection, we find quite puzzling the recent results of [13] where the authors claim a very strong sensitivity of the ηd scattering to the contribution of π -exchange, which visibly weakens the strength of the ηd attraction and results in a drastic reduction of the elastic cross section. The effect of pion exchange in ηd elastic scattering as predicted by our model is shown in Fig. 2. In contrast to [13], it is positive and quite small. One essential distinction from our work is that very different cut-off parameters $\beta_{N^*}^{(\eta)} \approx 13 \text{ fm}^{-1}$ and $\beta_{N^*}^{(\pi)} = 1.2 \text{ fm}^{-1}$ are used in [13]. One could suspect that in this case the πN -force may become important due to its relatively long-range nature. In order to check the sensitivity of the results to the choice of the meson-nucleon cut-offs we have performed a calculation with a new set of N^* -parameters including the same cut-off parameters as in [13]

$$g_{N^*}^{(\eta)} = 2.13, \quad g_{N^*}^{(\pi)} = 3.8, \quad \beta_{N^*}^{(\eta)} = 13 \text{ fm}^{-1}, \quad \beta_{N^*}^{(\pi)} = 1.2 \text{ fm}^{-1}, \quad M_0 = 1656 \text{ MeV}. \quad (49)$$

In this case, without pion exchange one observes a reduction of the total cross section by about 30% close to zero energy and by about 10% at $E_{\eta d} = 20 \text{ MeV}$, which remains much different to the results of [13].

At this point one may speculate about another possible explanation: A further distinction from our work is, that in [13] nonrelativistic kinematics for all participating particles was used. In this case, in going from η - to π -exchange one finds in the expression of the denominator of the driving term $Z_{N^*N^*}^{(\pi)}(W, \vec{p}', \vec{p})$ (see (9), (10) and (29)) an additional mass difference $M_\eta - M_\pi$, i.e.

$$W - E_N(\vec{p}_i) - E_N(\vec{p}_j) - \sqrt{(\vec{p}_i + \vec{p}_j)^2 + M_\pi^2} \rightarrow E + M_\eta - M_\pi - \frac{p_i^2}{2M_N} - \frac{p_j^2}{2M_N} - \frac{(\vec{p}_i + \vec{p}_j)^2}{2M_\pi}, \quad (50)$$

with $E = W - 2M_N - M_\eta$. Examining the formalism in [9] and [13], one possibility could be that this term was absent in the calculation. It is clear that the mass difference shifts effectively the on-shell kinetic energy to higher values, $E \rightarrow E + M_\eta - M_\pi \gg E$, so that only the less important high momentum part of the N^*N -interaction becomes sensitive to π -exchange.

(iv) In order to show to which extent the first order rescattering terms alone take into account the rescattering effect, we have also plotted their contributions to the Argand plots and have presented the corresponding cross section in Fig. 2. We see that the major contributions beyond the first order terms are the ones to the $L = 0$ partial wave amplitude. This is consistent with our intuitive expectation that the higher order terms in a multiple scattering series involve essentially the short distances in the interacting system, which contribute mostly to the s -wave part. This fact is demonstrated by the Argand plots, where we see that the s -wave amplitude is very poorly represented by the first order term. In the region $E_{\eta d} = 2 - 20$ MeV the letter goes beyond the unitary circle. On the other hand, the first order approximation is well justified for higher partial waves with $L = 1$ and 2. This effect is also partially explained by the specific features of our two-body input where only the s -wave orbitals are involved.

It would be useful to check the correct three-body results against those given by the optical model. This model, in the KMT version, was applied to the description of the final state interaction in the $\gamma d \rightarrow \eta d$ reaction [20]. Its crucial approximation is the neglect of target excitations in between scatterings. The domains within which this adiabatic idea is expected to work is, for example, pion scattering on medium and heavy nuclei. But it is not clear whether the optical picture is applicable to the ηNN -system, because of its nonadiabatic nature this approach may be too restrictive. Therefore, we consider here this approximation in order to establish the range of its validity and to understand its connection with such a fundamental model as the Faddeev theory. In order to arrive at the appropriate equations from our three-body ansatz (25)-(27), we neglect the terms, containing $Z_{N^*N^*}^{(\alpha)}$ and change also the function τ_d of (33) to the pure pole form

$$\tau_d = \frac{N_d^2}{E_{NN} + |\epsilon_d|}. \quad (51)$$

For the transition amplitude X_d , we then obtain the equation

$$X_d = V_d + \frac{1}{2}V_d\tau_d X_d, \quad (52)$$

where

$$V_d = 2Z_{dN^*} \tau_{N^*} Z_{N^*d} = \langle \phi_d | \sum_{i=1,2} t_{\eta N}(i) | \phi_d \rangle \quad (53)$$

is the familiar first order optical potential for ηd scattering. Following the authors of [20] we have introduced the additional factor 1/2 in (52) in order to avoid the double counting of the ηN -interaction. The s -wave amplitude $F_{\eta d}^0(q)$ obtained within this approach is also shown in Fig. 1. We see that the quality of the optical model prediction is rather poor notably near the scattering threshold. It underestimates distinctly the ηNN -interaction strength at low energies. Furthermore neglecting the excitation of the NN -subsystem breaks the three-body unitarity so that the corresponding inelasticity parameter exceeds unity. We may conclude that due to the limitations discussed above, the optical model is unable to incorporate the important properties of the ηNN interaction near threshold and is a rather bad approximation to the exact theory.

IV. BREAK UP CHANNELS AND UNITARITY

Up to now, the break up reactions $\eta d \rightarrow \eta np$ and $\eta d \rightarrow \pi NN$ have not been investigated in detail, one of the reasons being the much more complex calculations involved. The transition matrix element X_0 for the break up process $\eta d \rightarrow \eta np$ may easily be evaluated once the rearrangement amplitudes $X_d^{(\eta)}$ and X_{N^*d} in the ($S = 1, T = 0$) channel are calculated for the appropriate region of the final phase space. Then one has

$$X_0(W, \vec{p}_1, \vec{p}_2, \vec{q}, \vec{k}) = (f_{N^*}^{(\eta)}(\vec{p}_{\eta 1}) \tau_{N^*}(W_{N^*}) X_{N^*d}(W, \vec{p}_2, \vec{k}) + (1 \leftrightarrow 2)) + f_d(\vec{p}_{12}) \tau_d(W_d) X_d^{(\eta)}(W, \vec{q}, \vec{k}), \quad (54)$$

where the amplitudes X_{N^*d} and $X_d^{(\eta)}$ can be decomposed according to

$$X(W, \vec{p}, \vec{p}') = 4\pi \sum_L (2L + 1) X^L(W, p, p') P_L(\hat{p} \cdot \hat{p}'). \quad (55)$$

Here W denotes the total three-body c.m. energy and \vec{k} the momentum of the incident η -meson. The three-momenta of the final nucleons and the η -meson are denoted by \vec{p}_1 , \vec{p}_2 and \vec{q} , respectively. The arguments of the vertex functions $f_i(\vec{p})$ in (54) are the nonrelativistic two-body relative momenta, determined by the final state kinematics as ($i = 1, 2$)

$$\vec{p}_{\eta i} = \frac{M_N \vec{q} - m_\eta \vec{p}_i}{M_N + m_\eta}, \quad \vec{p}_{12} = \frac{1}{2}(\vec{p}_1 - \vec{p}_2). \quad (56)$$

The c.m. break up cross section is then given by

$$d\sigma(\eta d \rightarrow \eta np) = \frac{1}{(2\pi)^5} \frac{E_d(\vec{k}) M_N^2}{4Wk} N_d^2 |X_0(W, \vec{p}_1, \vec{p}_2, \vec{q}, \vec{k})|^2 d\Omega_\eta dE_\eta d\phi_{N_1} dE_{N_1}, \quad (57)$$

where the initial deuteron energy is $E_d(\vec{k}) = \sqrt{k^2 + M_d^2}$. The angle ϕ_{N_1} is the azimuthal angle of the nucleon momentum \vec{p}_1 relative to the \vec{k} - \vec{q} plane in the frame where the z -axis is chosen along \vec{q} . For the absorptive channel $\eta d \rightarrow \pi NN$, only the first two terms in (54) remain as follows from the spin-isospin selection rules.

Our predictions for the η -meson spectrum are shown in Fig. 3. Firstly, one observes a strong decrease of the cross section by the ηNN interaction of about 85 %. This effect may be explained, at least partially, by the orthogonality of the initial and final NN wave functions. Also within the first order rescattering approximation one finds a strong reduction of the IA, but the size of this effect is evidently underestimated, so that this approximation results in a cross section about a factor of 2 larger than the complete calculation.

The total cross sections for the elastic and inelastic channels are shown in Fig. 4. We see that the $\eta d \rightarrow \eta np$ cross section is in general small, also due to the damping effect noted above. On the other hand, the absorptive channel $\eta d \rightarrow \pi NN$ gives an essential part of the total cross section. This may be explained firstly by the relatively large phase space available for pion emission already at low initial kinetic energies. Secondly, the cross section diverges as $1/v$, where v is the ηd relative velocity, near the elastic scattering threshold, which is typical for exothermic reactions.

The break up processes provide us also with a check of the question whether the limitation to the lowest partial waves is justified by considering the unitarity relation, which couples these channels to the elastic one. An important consequence from this relation is the well known optical theorem, which in our case reads

$$\frac{4\pi}{q} \Im m F_{\eta d}(\theta = 0) = \sigma_{tot} = \sigma(\eta d \rightarrow \eta d) + \sigma(\eta d \rightarrow \eta np) + \sigma(\eta d \rightarrow \pi NN). \quad (58)$$

Thus a comparison of both sides of this relation allows one to estimate how crucial the truncation of the partial wave expansion is. Furthermore, this is also a natural method to check the accuracy of the numerical procedure applied for solving the basic equations (25)-(27). To this end we have calculated both sides of (58) and present in Fig. 5 the relative deviation

$$R = \frac{\frac{4\pi}{q} \Im m F_{\eta d}(\theta = 0) - \sigma_{tot}}{\sigma_{tot}}. \quad (59)$$

The fact, that $|R|$ does not exceed 2% over the whole energy range considered, gives us confidence that the approximations of the present approach are not crucial and that our results are well founded. But one has to keep in mind that at higher energies the neglected higher partial waves have to be included and very likely also the two-pion channel which has been neglected completely in this work.

V. η -PHOTOPRODUCTION ON THE DEUTERON

We now will turn to η -production reactions which are more easily accessible in an experiment. Our main concern will be to see to what extent the strong final-state ηNN -interaction will influence the dynamical properties of such reactions and what type of information on the N^*N -interaction can be extracted from them. Most interesting are the coherent and incoherent η -photoproduction processes $\gamma d \rightarrow \eta d$ and $\gamma d \rightarrow \eta np$ which, for the reasons noted in the introduction, were extensively investigated both theoretically and experimentally during recent years.

As usual, we treat the electromagnetic interaction in first order perturbation theory. To apply the formalism represented by the system in (25)-(27) to the η -photoproduction, one just has to replace the η -meson by the photon in the entrance channel. This then yields a set of coupled equations which are formally similar to (25)-(27) but where the driving interaction in (25) has been changed according to

$$Z_{N^*d}^{(\eta)} \rightarrow \langle N^*(\gamma) | G_{\gamma NN} | d \rangle, \quad (60)$$

where $G_{\gamma NN}$ denotes the free propagator in the γNN -sector and $|N^*(\gamma)\rangle$ the electromagnetic vertex function for the transition $\gamma N \rightarrow N^*$. The method of inversion of the corresponding three-particle equations, described in the Appendix, remains of course the same. For the electromagnetic vertex $|N^*(\gamma)\rangle$ we use the parametrization

$$\langle \vec{p} | N^*(\gamma) \rangle = g_{\gamma NN^*}^{(N)} \frac{\beta_{N^*}^{(\gamma)2}}{\beta_{N^*}^{(\gamma)2} + k_{\gamma N}^2}, \quad (61)$$

where $k_{\gamma N}$ is the γN c.m. momenta and $\beta_{N^*}^{(\gamma)}$ was taken to be 480 MeV. In the proton channel the value $g_{\gamma NN^*}^{(p)}$ was determined by fitting the experimental $\gamma p \rightarrow \eta p$ cross section [33]. For the neutron channel we have used the relation $g_{\gamma NN^*}^{(n)} = -0.80 g_{\gamma NN^*}^{(p)}$ which is compatible with different analyses [17,21,34]. In principle, there is a complex phase between the proton and neutron amplitudes as has been pointed out in [24]. However, the incoherent reaction is not sensitive to this phase and thus its neglect is not crucial there. On the other hand, this phase is important for the strength of the isoscalar part of the amplitude which determines completely the coherent reaction. This is discussed below in Sect. V A.

Keeping in mind the discussion given in Sect. III, we can expect that the higher order terms of the multiple scattering series are important only for the lowest partial waves of the transition amplitude and have very little effect on the higher partial waves. This allows us to treat the latter perturbatively by taking into account the first order rescattering terms only. This may easily be done by adding and subtracting the first order rescattering amplitude from that given by the full three-body calculation. Schematically we may write

$$X = X^{resc} + (X - X^{resc}). \quad (62)$$

The first term can be calculated directly using the cartesian basis without making a partial wave decomposition. The corresponding techniques have been described before, e.g., in [23,35,36], and need not be repeated here. The second term in (62) converges very rapidly to zero for the higher partial waves, so that only the contribution from the $L = 0$ part has to be taken into account.

In the γd c.m. system, the cross sections for the coherent and incoherent photoproduction reactions are

$$d\sigma(\gamma d \rightarrow \eta d) = \frac{q}{k} \frac{E_d(\vec{k}) E_d(\vec{q})}{(4\pi W)^2} \frac{N_d^2}{6} \sum_{\text{spins}} |X_d^{(\eta)}(W, \vec{q}, \vec{k})|^2 d\Omega_\eta, \quad (63)$$

$$d\sigma(\gamma d \rightarrow \eta np) = \frac{1}{(2\pi)^5} \frac{E_d(\vec{k}) M_N^2}{4W k} \frac{N_d^2}{6} \sum_{\text{spins}} |X_0(W, \vec{p}_1, \vec{p}_2, \vec{q}, \vec{k})|^2 d\Omega_\eta dE_\eta d\phi_{N_1} dE_{N_1}, \quad (64)$$

where all notations are the same as in (57) with \vec{k} being the photon momentum.

From the results obtained for ηd -scattering we can expect that the strong ηNN -interaction will appreciably influence the observables of η -photoproduction, too. Indeed, the strong attraction in the ηNN -system, already mentioned above, tends to hold the participating particles in the region where the primary ‘‘photoproduction interaction’’ works. Since the rate of the $(\gamma \rightarrow \eta)$ -transition will be proportional to the probability of finding the produced η in this region, a strong enhancement of the η -production cross section may be expected near threshold [37].

A. Coherent η -photoproduction on the deuteron

The coherent channel $\gamma d \rightarrow \eta d$ has been investigated theoretically rather extensively in contrast to very few reliable experimental data reflecting the enormous difficulty for separating this small cross section from the dominant incoherent reaction. One of the most important questions in relation to the coherent photoproduction is the isotopical separation of the $\gamma N \rightarrow N^*$ amplitude as already pointed out above. Recent work [24] has shown that the consideration of the relative phase between the proton and neutron N^* -photoexcitation amplitudes is very essential. Consequently, it is practically impossible to extract the isoscalar part $g_{\gamma NN^*}^{(s)}$ of the $\gamma N \rightarrow N^*$ amplitude from the observation of only $\gamma p \rightarrow \eta p$ and $\gamma d \rightarrow \eta np$ reactions. The model dependent fixing of this phase may be done, e.g., by the analysis of the multipole pion photoproduction amplitudes, as in [24,38]. Since this question is beyond the scope of the present paper, we treat the modulus of the isoscalar part of the amplitude as a free parameter. Our predictions for the total $\gamma d \rightarrow \eta d$ cross section obtained with

$$\alpha = \left| \frac{g_{\gamma NN^*}^{(s)}}{g_{\gamma NN^*}^{(p)}} \right| = 0.26 \quad (65)$$

are presented in Fig. 6. One readily notes that the strong attraction in the ($S = 1, T = 0$)-channel reflects itself in a drastic increase of the cross section over a mere IA-calculation just above threshold. It is worth mentioning that the experimental confirmation of this result, i.e., the observation of the strong enhancement of the η -yield close to the threshold would imply that the present theoretical ideas on the ηNN low-energy dynamics are substantially correct. In view of the strong s-wave dominance in the $\gamma d \rightarrow \eta d$ cross section near threshold, we may expect an important influence of the higher order rescattering terms. As is demonstrated in Fig. 6, taking into account only first order rescattering, we are not able to reproduce neither the common trend nor the size of the results given by the complete calculation. Compared to the recent work of [24], the present results confirm the inadequacy of the first order rescattering. However, the energy dependence of the total cross section differs substantially from those of [24]. This difference is of course a consequence of the present three-body approach to the ηNN -system which was beyond the scope of [24].

Another feature which deserves a comment is that, due to the large momentum transfer associated with the large η -mass, the high momentum part of the N^*N -interaction becomes important already near threshold. The latter leads to the increase of the π -exchange contribution which was found to be almost negligible in ηd -scattering (see the discussion in Sect. III). As we can see, the general effect of including the π -exchange is to enhance the near-threshold cross section by more than a factor 1.2. This sensitivity of the $\gamma d \rightarrow \eta d$ reaction to the pion contribution was also noted in [24]. We must furthermore mention that the importance of the N^*N rearrangement potential $Z_{N^*N^*}$ (48) in the π - and η -channels depends strongly on the strength of the ηNN^* and πNN^* couplings used.

In comparison with the results of [10], we firstly would like to emphasize once more that in our case the source of the strong final state interaction is the virtual ηNN s-wave pole found in [12]. Therefore it is not surprising that our theory leads to substantially different results than those of [10] where the s-wave ηd -resonance governs the whole reaction dynamics. In particular, we found no evidence from the resonant peak in the total cross section at $E_\gamma = 635$ MeV. It should also be noted that the effect of ηd -interaction obtained by us, although being essential, is however not as strong as predicted in the pioneering work [19].

In Fig. 7 we show our results for the differential cross section at two photon energies. Analyzing the influence of the ηNN -interaction we conclude that the final state interaction tends to enhance the s-wave part of the reaction amplitude and thus to make the angular distribution somewhat more isotropic. The magnitude of the available experimental data [21] covering the near-threshold region is not reproduced with $\alpha = 0.26$ but one must note that the results of the most recent measurements [39,40] are consistent with this value of α .

B. Incoherent channel $\gamma d \rightarrow \eta np$

With respect to the incoherent η -photoproduction on the deuteron, there exist fewer theoretical studies as for the coherent reaction. In our previous work on $\gamma d \rightarrow \eta np$ [14,23], we have addressed the effects of final state rescattering. Besides the investigation of the main properties of the cross section in the near threshold region, we have studied in particular the importance of three-body dynamics in the final ηnp system. It has been shown that a restriction to the first order rescattering with respect to the NN - and ηN -final state interaction does not give a sufficiently accurate approximation to the s-wave reaction amplitude and that higher order terms make very substantial contributions. At this point we would like to note that the numerical results in [14] contained an error. The correct calculation presented here yields somewhat larger predictions. In this work, we also would like to complement our previous studies.

As first, we show in Fig. 8 the angular distribution of the outgoing meson, calculated in the c.m. system at the energy 5 and 15 MeV above threshold. One readily sees that the strong attraction in the s-wave ($S = 0, T = 1$) state implies a substantial enhancement over the IA cross section while making the angular distribution rather isotropic. As was already discussed in our previous paper [14], the first order rescattering is unable to describe close to threshold the size of the cross section obtained within the three-body formalism.

The importance of the ηNN -interaction for the η -photoproduction reaction is most apparent in the total cross section exhibited in Fig. 9. It was shown in [23] that the impulse approximation (IA) is strongly suppressed because of the large spectator nucleon momenta required for the production of a low-energy η -meson in this approximation. In contrast to the IA, the complete three-body approach results in a cross section which exhibits a strong enhancement starting right from threshold. Therefore, the observed rather high values of the η -meson yield near threshold are explained in principle. Adding the contribution from the coherent channel, we obtain the inclusive cross section $\sigma(\gamma d \rightarrow \eta X) = \sigma(\gamma d \rightarrow \eta np) + \sigma(\gamma d \rightarrow \eta d)$ which was actually measured in the experiment [17]. One readily notices, that in this region our theoretical predictions are in reasonable agreement with the data.

In the same figure we demonstrate the role of pion exchange in the break-up channel. The dash-dotted curve shows the results obtained when the terms containing $Z_{N^*d}^{(\pi)}$, $Z_{dN^*}^{(\pi)}$ and $Z_{N^*N^*}^{(\pi)}$ in equations (25) through (27) are neglected. In this case, in contrast to the coherent reaction, the role of the neglected terms appears to be rather small. This is

due mainly to the fact that the pion exchange potential $Z_{N^*N^*}^{(\pi)}$ in the $T = 1$ channel is three times weaker than in the $T = 0$ state. The role of the other two terms $Z_{N^*d}^{(\pi)}$ and $Z_{dN^*}^{(\pi)}$, which do not contribute to the coherent process, turns out to be totally negligible.

Here we would like to note that our primary goal was to treat as precisely as possible the three-body aspects of the problem, which requires, of course, a few simplifications of some model ingredients. In particular, we have neglected here the tensor NN -force and consequently the D-wave component of the deuteron wave function. As was shown in [23], due to the large momentum transfer, the contribution arising from the D-wave part of the deuteron shows up near threshold and reduces the pure S-wave cross section sizeably. Therefore, a more refined analysis should be based on a more realistic deuteron wave function.

VI. CONCLUSIONS AND OUTLOOK

In the present paper, which we consider as an exploratory step towards a quantitative understanding of the dynamical properties of the ηNN -interaction at low energy, we have shown that in view of the relatively strong attraction, both in the ηN - and NN -subsystems, the appropriate theoretical framework is given by the three-body scattering approach of Faddeev type. It allows one to include all orders of the rescattering expansion systematically. We were interested mainly in the energy region of low kinetic energies with particular emphasis on the first few MeV above the ηd -scattering threshold, which is of special interest for η -nuclear studies. Our main results may be summarized as follows:

(i) In the low-energy regime, the major contributions of higher order rescattering beyond the first order term appear in the $L = 0$ partial wave. This observation is consistent with the notion that higher order terms involve mainly short distances in the deuteron. Our explicit study shows that for the higher partial waves there is no need to invert the three-body equations, since the corresponding Neumann series converges very rapidly, so that only the first nontrivial term is sufficient in order to take into account rescattering effects in these partial waves.

(ii) The importance of rescattering in the inelastic channel $\eta d \rightarrow \eta np$ is a necessary consequence of the orthogonality of the initial and final NN -states. We have shown that this effect largely reduces the probability of the deuteron break up in the allowed kinematical domain.

(iii) The ηNN dynamics, as manifest in the photon induced reactions $\gamma d \rightarrow \eta d$ and $\gamma d \rightarrow \eta np$, is to some extent unrelated to the on-shell ηd -interaction. In particular, the exchange of retarded pions, which is found to be negligible in elastic scattering, becomes much more pronounced in the coherent photoproduction process because of the increased importance of the high momentum components of the N^*N -interaction.

(iv) The exact treatment of the three-body aspects of the ηNN final state in the η -photoproduction on a deuteron is quite essential for a quantitative understanding of the form as well as the size of the angular distributions of produced etas. The general effect of the ηNN -interaction is to enhance the s -wave part of the scattering amplitude close to the production threshold. As a consequence, we found a distinct shift of the major part of the η -meson yield to the low-energy region as well as a rather isotropic character of the corresponding angular distributions.

Finally, we would like to make a few remarks with respect to the use of the developed theory for η -photoproduction on heavier nuclei. Firstly, we would like to recall that close to threshold this reaction is accompanied by a large momentum transfer Δp in the whole region of available emission angles. On the other hand, the energy ΔE deposited into the nucleus is minimal, such that

$$\Delta E \ll \frac{(\Delta p)^2}{2M_N}. \quad (66)$$

Therefore, one may expect that the single particle response preferring the “quasifree” kinematics, where

$$\Delta E \approx \frac{(\Delta p)^2}{2M_N}, \quad (67)$$

must be strongly suppressed. We have already observed this effect in the reaction $\gamma d \rightarrow \eta np$, where a strong suppression of the IA-contribution was found. Thus in this situation the mechanism where two or more nucleons are allowed to share the transferred momentum becomes important. As the dominant reaction mode we thus may assume a two-nucleon response where the η -meson is produced on a correlated pair of nucleons. The case of three or more participating particles requires the presence of more than two nucleons close together which seems to be less probable. Furthermore, the strong attraction of the ηNN -system as found in the present work tends to hold it together, so that the production of a strongly correlated NN^* -pair and its decay into the ηNN -channel may appear to be the most important mechanism for η -photoproduction on nuclei near threshold. Taking into account these qualitative arguments, we may conclude that our approach may also be useful for the study of η -photoproduction on complex nuclei.

ACKNOWLEDGMENTS

A.F. is grateful to the theory group for the kind hospitality during his stay at the Institute of Nuclear Physics of the University of Mainz.

APPENDIX: METHOD OF SOLUTION

In order to solve the equations (25)-(27), we use the method of contour deformation developed mainly in [41] for elastic scattering and extended for break-up processes in [42]. We will not give any details at this point and consider only that part of the formalism, which is connected with relativistic kinematics which is not touched upon in the literature to the best of our knowledge. The method was developed to avoid the problems, caused by the moving logarithmic singularities in the terms $Z_{ij}^L(W, q', q)$. As is well known, these singularities arise from the exchange of a particle with positive kinetic energy. Above the inelastic threshold (in our case we have two inelastic thresholds – πNN at $W \approx 2017$ MeV and ηNN at $W \approx 2425$ MeV), Z_{ij}^L contains a right-hand cut and, as a consequence, becomes complex, where the imaginary part is as usually determined by the discontinuity across the cut. As an example, let us consider a driving term Z_{ij}^L of the general form

$$Z_{ij}^L(W, q', q) = \frac{1}{8\pi} \int_{-1}^1 \frac{f_i^*(\vec{p}_1(\vec{q}', \vec{q})) f_j(\vec{p}_2(\vec{q}', \vec{q}))}{W - E_i(\vec{q}') - E_j(\vec{q}) - \sqrt{(\vec{q}' + \vec{q})^2 + M_k^2} + i\epsilon} P_L(\hat{q}' \cdot \hat{q}) d(\hat{q}' \cdot \hat{q}), \quad i, j, k \in \{d, N^*\}. \quad (\text{A1})$$

The main types of singularities of Z_{ij}^L as a function of q for three different regions of the momentum q' are shown in Fig. 10. For the boundary values of q' one finds

$$q'_1 = \frac{\lambda^{1/2}((W - M_j)^2, M_i^2, M_k^2)}{2(W - M_j)} \quad (\text{A2})$$

$$q'_2 = \frac{\lambda^{1/2}(W^2, M_i^2, (M_j + M_k)^2)}{2W}, \quad (\text{A3})$$

where the triangle function $\lambda(x, y, z)$ has the form (see, e.g., [43])

$$\lambda(x, y, z) = (x - (\sqrt{y} + \sqrt{z})^2) (x - (\sqrt{y} - \sqrt{z})^2). \quad (\text{A4})$$

The position of the logarithmic poles q_1 and q_2 can easily be found to be

$$q_1 = \frac{\alpha q' + D}{W_i^2}, \quad (\text{A5})$$

$$q_2 = \left\{ \begin{array}{l} \frac{-\alpha q' + D}{W_i^2}, \quad \text{for } q' < q'_1 \\ \frac{\alpha q' - D}{W_i^2}, \quad \text{for } q' > q'_1 \end{array} \right\}, \quad (\text{A6})$$

where W_i is defined in (7) and

$$\alpha = \frac{1}{2}(M_j^2 - M_k^2 + W_i^2), \quad (\text{A7})$$

$$D = (W - E_i(\vec{q}')) \sqrt{\alpha^2 - M_j^2 W_i^2}. \quad (\text{A8})$$

Also shown in Fig. 10 is the deformed contour C along which $Z_{ij}^L(W, q', q)$ as a function of q for fixed q' has no singularities so that the equations (25)-(27) may be solved by matrix inversion. The solutions for real values of q' may be obtained by the one-fold iteration of the same equations along the real axis q . In the case of pure elastic processes, such as $\eta d \rightarrow \eta d$ and $\gamma d \rightarrow \eta d$, only the case (a) may be realized and the iteration becomes trivial. Some problems arise for the break up processes $\eta d \rightarrow \eta np$ and $\gamma d \rightarrow \eta np$, where also the case (b) is realized in the appropriate region of q' . In this case, the knowledge of the amplitude X in the interval $[0, q_2]$ is needed. By direct manipulation, one can see that the inequality $q'_{1 \min} > q_2$ always holds. Here $q'_{1 \min}$ is the minimal value from the boundary momenta q'_1 obtained according to (A2)-(A3) for all potentials Z_{ij} involved in our dynamical equations (25) – (27). Therefore,

the needed values of the X -matrix are always known and the case (b) leads only to a non-essential calculational complexity. In this case the iteration is carried out according to the formula (omitting the spin-isospin notations)

$$Z_{ij}^L \tau_j X_j^L = \frac{2}{\pi} \int_0^{q_2} Disc [Z_{ij}^L(W, q', q'')] \tau_j(W_j) X_j^L(W, q'', q') \frac{q''^2 dq''}{\epsilon_j(q'')} + \frac{2}{\pi} \int_C Z_{ij}^L(W, q', q'') \tau_j(W_j) X_j^L(W, q'', q') \frac{q''^2 dq''}{\epsilon_j(q'')}, \quad (\text{A9})$$

where, as one can prove using the definitions of (10) and (41)

$$Disc [Z_{ij}^L(W, q', q'')] = i\pi \frac{g_i g_j \beta_i^2 \beta_j^2}{16\pi} \frac{M_k^2}{\mu_i \mu_j} \frac{P_L(x_0)}{(q' q'')^3 (a_i + x_0)(a_j + x_0)}, \quad (\text{A10})$$

with

$$x_0 = \frac{(W - E_i(q') - E_j(q''))^2 - M_k^2 - q'^2 - q''^2}{2q' q''}, \quad (\text{A11})$$

$$a_i = \frac{M_k}{2q' q'' \mu_i} (\beta_i^2 + q''^2 + (q' \mu_i / M_k)^2), \quad (\text{A12})$$

$$a_j = \frac{M_k}{2q' q'' \mu_j} (\beta_j^2 + q'^2 + (q'' \mu_j / M_k)^2). \quad (\text{A13})$$

It is important that when integrating along the contour C in the case (b) one has to go into the second sheet (dashed line between the points 0 and q_B in Fig. 10). In the case (c) $q' > q'_2$, the singularities are shifted into the complex plane and therefore do not cause any problems.

In conclusion we would like to note, that the kinematical area in which the case (b) is realized is rather small. As the direct calculation shows, the neglect of the first term in (A9) does not lead to any markable change of the results.

- [1] H.C. Chiang, E. Oset, and L.C. Liu, Phys. Rev. C **44**, 738 (1991).
- [2] M. Kohno and H. Tanabe, Nucl. Phys. A **519**, 755 (1990).
- [3] R.S. Carrasco, Phys. Rev. C **48**, 2333 (1993).
- [4] B.V. Krippa and J.T. Londergan, Phys. Rev. C **48**, 2967 (1993).
- [5] A. Hombach, A. Engel, S. Teis, and U. Mosel, Z. Phys. A **352**, 223 (1995).
- [6] T. Ueda, Phys. Rev. Lett. **66**, 297 (1991).
- [7] A.M. Green and S. Wycech, Phys. Rev. C **55**, 2167 (1997).
- [8] N.V. Shevchenko, V.B. Belyaev, S.A. Rakityansky, S.A. Sofianos, and W. Sandhas, Eur. Phys. J. A **9**, 143 (2000).
- [9] H. Garcilazo and M.T. Peña, Phys. Rev. C **61**, 064010 (2000).
- [10] N.V. Shevchenko, V.B. Belyaev, S.A. Rakityansky, S.A. Sofianos, and W. Sandhas, Talk at the IX International Seminar "Electromagnetic interactions of nuclei at low and medium energies", Moscow, September 2000, nucl-th/0011027.
- [11] S. Wycech and A.M. Green, Nucl. Phys. A **663&664**, 529c (2000).
- [12] A. Fix and H. Arenhövel, Eur. Phys. J. A **9**, 119 (2000).
- [13] H. Garcilazo and M.T. Peña, Phys. Rev. C **63**, 021001 (2001).
- [14] A. Fix and H. Arenhövel, Phys. Lett. B **492**, 32 (2000).
- [15] R.S. Bhalerao and L.C. Liu, Phys. Rev. Lett. **54**, 865 (1985).
- [16] M. Batinic, I. Slaus, A. Svarc, and B. Nefkens, Phys. Rev. C **51**, 2310 (1995).
- [17] B. Krusche *et al.*, Phys. Lett. B **358**, 40 (1995).
- [18] V. Metag, Talk at the Baryon-98 conference, Bonn, September 1998.
- [19] T. Ueda, Phys. Lett. **B291**, 228 (1992).
- [20] S.S. Kamalov, L. Tiator, and C. Bennhold, Phys. Rev. C **55**, 98 (1997).
- [21] P. Hoffmann-Rothe *et al.*, Phys. Rev. Lett. **78**, 4697 (1997).
- [22] E. Breitmoser and H. Arenhövel, Nucl. Phys. A **612**, 321 (1997).
- [23] A. Fix and H. Arenhövel, Z. Phys. A **359**, 427 (1997).
- [24] F. Ritz and H. Arenhövel, nucl-th/0011089.
- [25] C. Lovelace, Phys. Rev. **135**, B1225 (1964).

- [26] I.R. Afnan and A.W. Thomas, Phys. Rev. C **10**, 109 (1974).
- [27] T. Ueda, Phys. Lett. B **141**, 157 (1984).
- [28] K. Miyagawa, T. Ueda, T. Sawada, and S. Takagi, Nucl. Phys. A **459**, 93 (1986).
- [29] Y. Yamaguchi, Phys. Rev. **95**, 1628 (1954).
- [30] M. Batinic, I. Slaus, A. Svarc, B. Nefkens and T.-S.H. Lee, Phys. Scr. **58**, 15 (1998).
- [31] A.R. Edmonds, *Angular Momentum in Quantum Mechanics* (Princeton University Press, Princeton, New Jersey, 1957).
- [32] M. Roebig-Landau *et al.*, Phys. Lett. B **373**, 45 (1996).
- [33] B. Krusche *et al.*, Phys. Rev. Lett. **74**, 3736 (1995).
- [34] V. Hejny *et al.*, Eur. Phys. J. A **6**, 83 (1999).
- [35] N. Hoshi, H. Hyuga, and K. Kubodera, Nucl. Phys. A **324**, 234 (1979).
- [36] D. Halderson and A.S. Rosenthal, Nucl. Phys. A **501**, 856 (1989).
- [37] K.M. Watson, Phys. Rev. **88**, 1163 (1952).
- [38] C. Bennhold and H. Tanabe, Nucl. Phys. A **530**, 625 (1991).
- [39] V. Metag, Talk at the Baryon-98 conference, Bonn, September 1998
- [40] J. Weiss, PhD Thesis, University of Giessen (2000).
- [41] J.H. Hetherington and L.H. Schick, Phys. Rev. **137**, B935 (1965).
- [42] R. Aaron and R.D. Amado, Phys. Rev. **150**, 857 (1966).
- [43] E. Byckling and K. Kajantie, *Particle Kinematics* (John Wiley & Sons, N.Y., 1973).

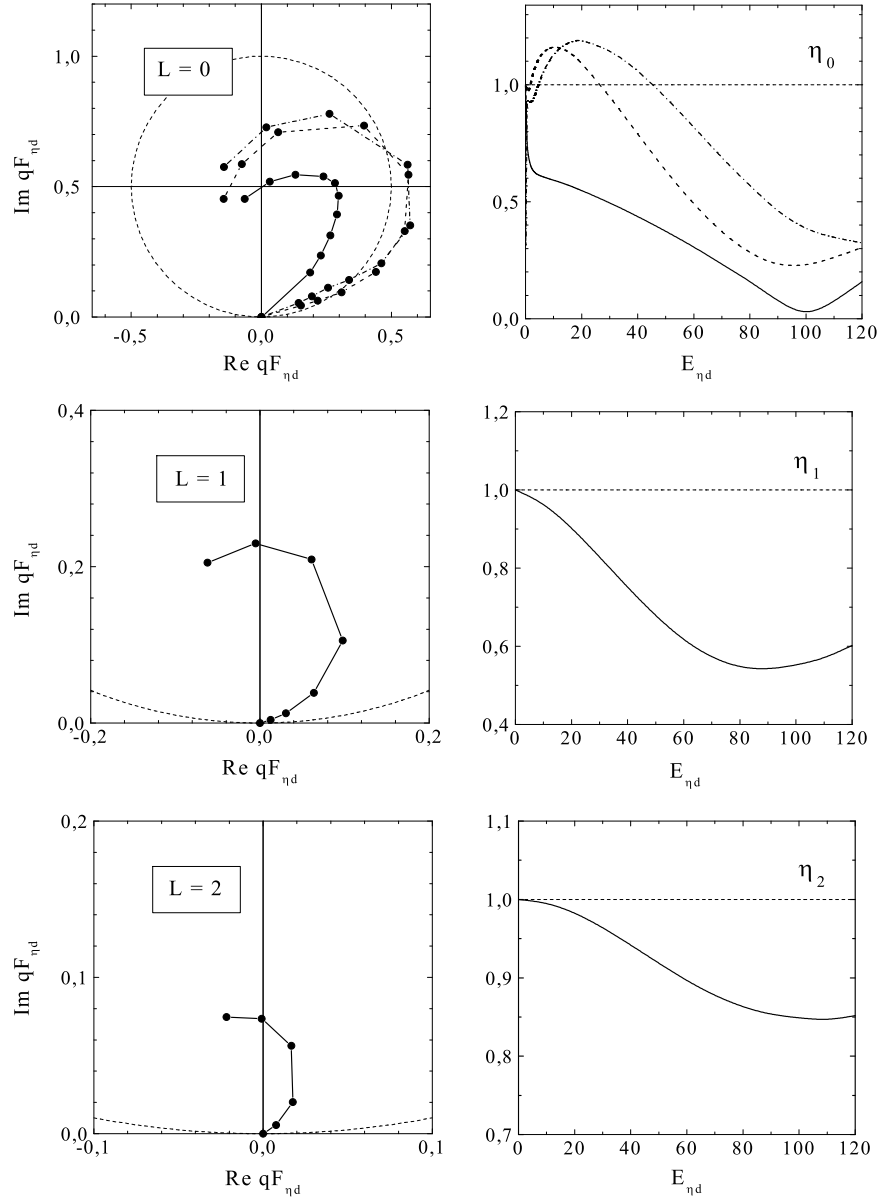


FIG. 1. Argand diagrams (left panels) and inelasticity parameters (right panels) for elastic ηd -scattering for the lowest ηd partial waves $L = 0, 1$, and 2 as a function of the c.m. kinetic energy $E_{\eta d}$. The dots mark the following energies for $L = 0$: $E_{\eta d} = 0, 0.5, 1, 2, 4, 8, 16, 32, 64, 90, 120$ MeV; for $L = 1$: $E_{\eta d} = 0, 4, 8, 16, 32, 64, 90, 120$ MeV; and for $L = 2$: $E_{\eta d} = 0, 16, 32, 64, 90, 120$ MeV; For $L = 0$, the dashed curve shows the result from the first order rescattering approximation and the dash-dotted one the result of the optical model. For the other partial waves, the first order rescattering approximation coincides essentially with the complete calculation.

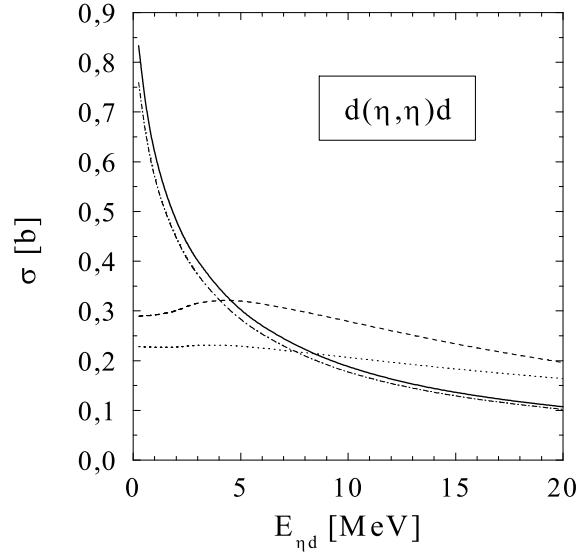


FIG. 2. Elastic ηd -total cross section versus the c.m. kinetic energy $E_{\eta d}$ for various theoretical ingredients. Notation of the curves: dotted: IA; dashed: first order rescattering; solid: complete three-body calculation; dash-dotted: three-body calculation but without π -exchange contribution to the driving term $Z_{N^*N^*}$.

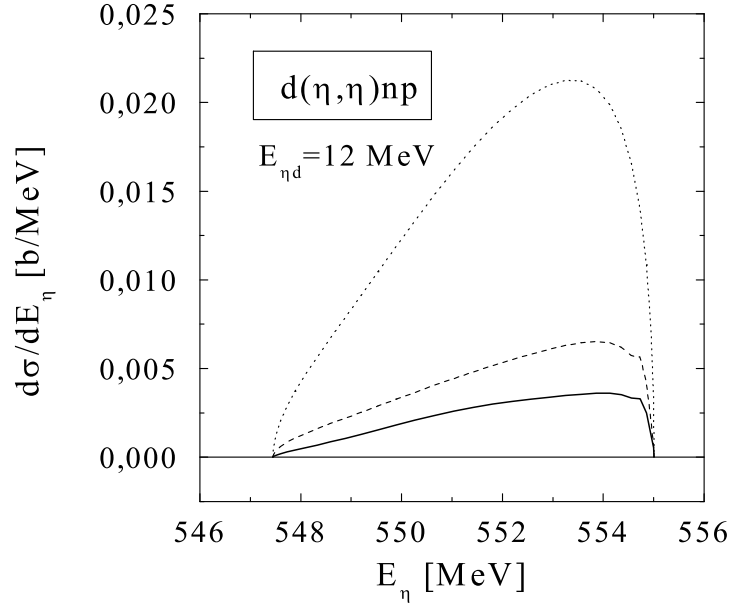


FIG. 3. Spectrum of the emitted η -mesons in inelastic ηd scattering calculated in the ηd c.m. system for an initial c.m. kinetic energy $E_{\eta d}=12$ MeV. Notation of the curves: dotted : IA; dashed: first order rescattering; solid: complete three-body calculation.

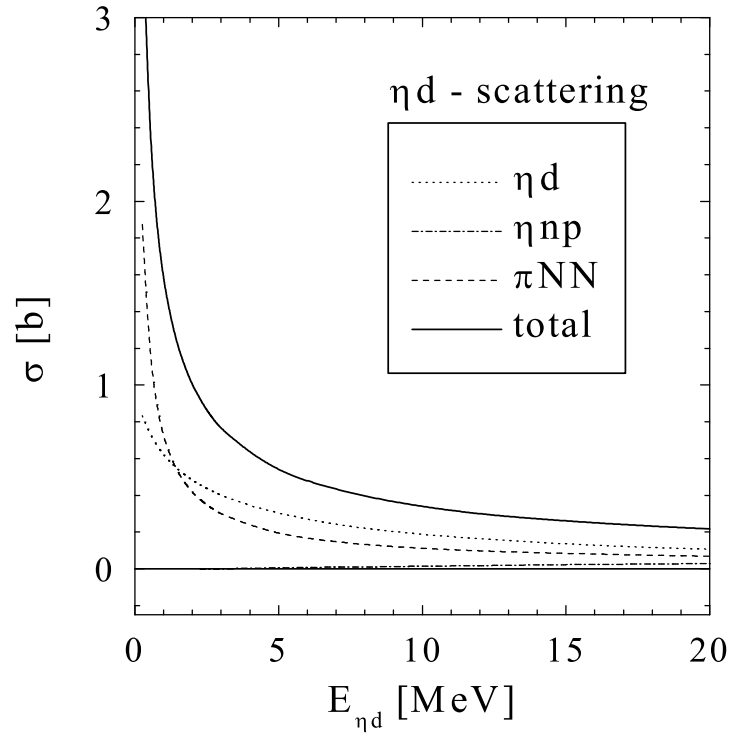


FIG. 4. Various contributions to the total ηd -cross section from the different channels. The solid curve shows the sum of all channels.

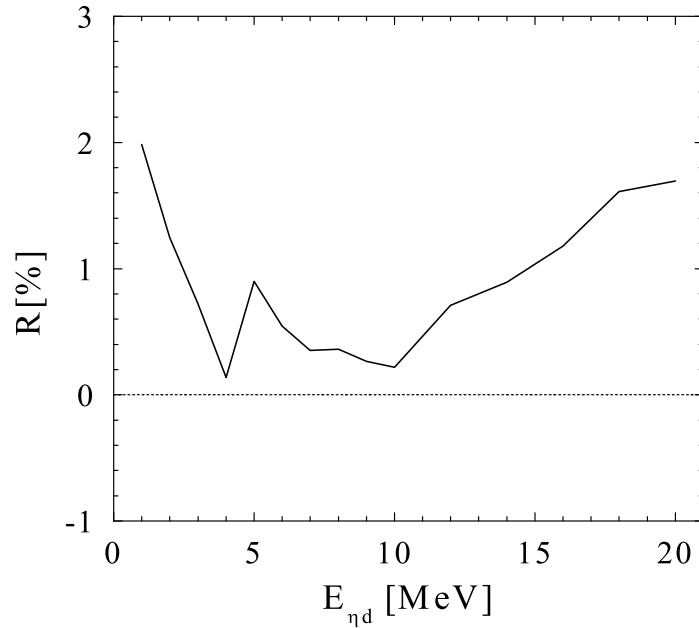


FIG. 5. Relative deviation R between the total cross sections calculated either explicitly from summing the various reaction channels or from the optical theorem (see definition in (59)).

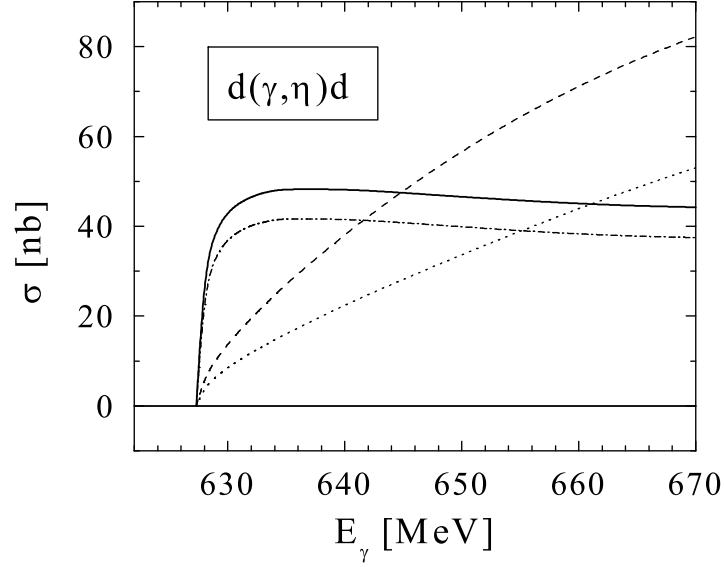


FIG. 6. Total cross section for the coherent reaction $\gamma d \rightarrow \eta d$. Notation of the curves: dotted: IA; dashed: first order rescattering; solid: complete three-body calculation; dash-dotted: three-body calculation without π -exchange contribution.

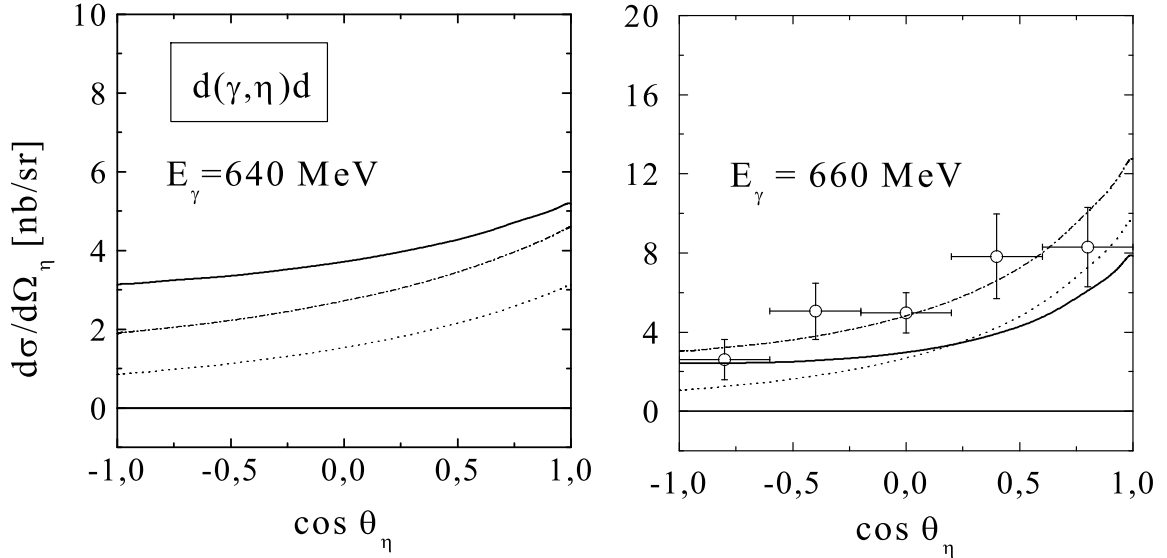


FIG. 7. Differential cross section for the coherent reaction $\gamma d \rightarrow \eta d$ in the γd c.m. system at two lab photon energies $E_\gamma = 640$ and 660 MeV. Notation of the curves: dotted: IA; dashed: first order rescattering; solid: complete three-body model. The open circles represent the data for an energy bin $E_\gamma = 652 - 664$ MeV from [21].

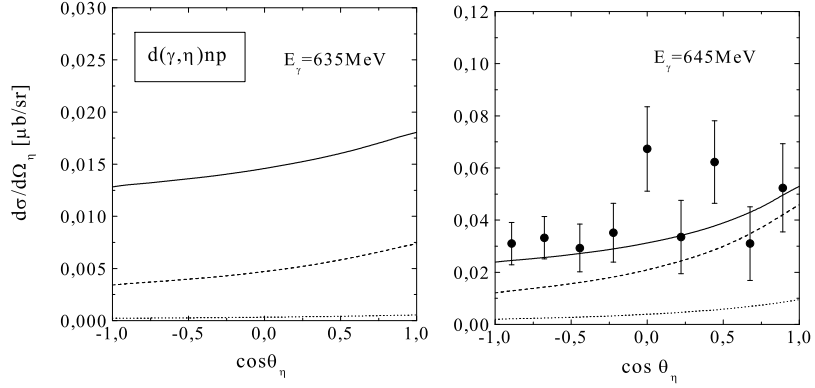


FIG. 8. Angular distribution of η -mesons of the incoherent reaction $\gamma d \rightarrow \eta np$ calculated in the γd c.m. system at the two lab photon energies. Notation of the curves as in 7. The experimental points are the inclusive $\gamma d \rightarrow \eta X$ measurements from [17].

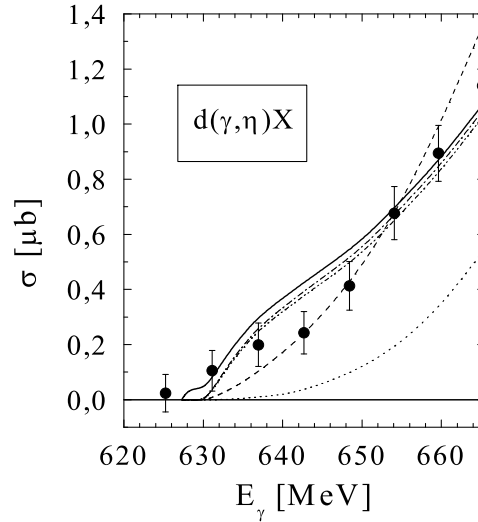


FIG. 9. Total cross section for the reaction $\gamma d \rightarrow \eta X$. Notation of the curves: dotted: IA; dashed: first order rescattering; dash-double-dot: complete the three-body model; dash-dot: three-body model without the contribution of π -exchange; solid: sum of coherent and incoherent channels. Inclusive $\gamma d \rightarrow \eta X$ data are taken from [17].

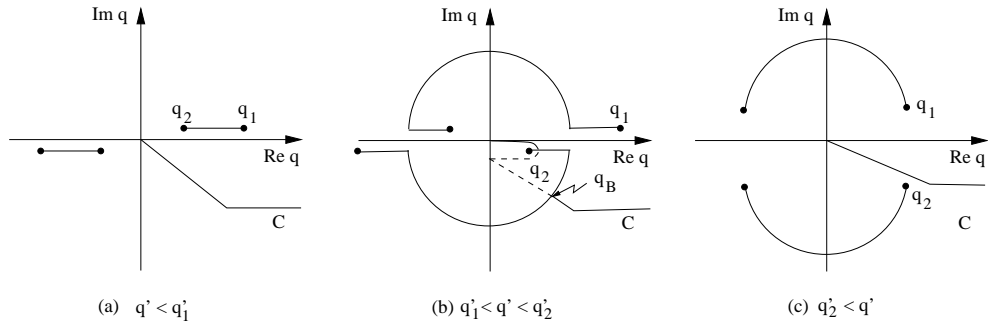


FIG. 10. Deformed integration path C and location of the cuts of the rearrangement potential $Z_{ij}(W, q', q)$ in the complex q -plane for three different regions of the momentum q' . Note that for case (b) the integration path crosses two times the cut so that in between C lies in the nonphysical sheet as indicated by the dashed line.